Earthquake Engineering, Tenth World Conference © 1992 Balkema, Rotterdam. ISBN 90 5410 060 5

Model tests of embankments on liquefiable ground using dynamic centrifuge

Y. Koga, J. Koseki & A. Takahashi
Public Works Research Institute, Tsukuba, Japan

ABSTRACT: Model tests were performed to study a seismic behavior of embankments on a liquefiable ground using dynamic centrifuge. Sinusoidal waves of a different frequency and two kinds of irregular waves were applied to the models as a shaking acceleration. Effects of the shape of the shaking acceleration on the excess pore pressure in the ground and on the settlement of the embankment were investigated, and the applicability of a cumulative damage concept in equalizing the irregular shaking wave was examined.

1 INTRODUCTION

Liquefaction of a sandy ground causes a settlement of an embankment founded on the ground. A lot of model tests have been executed to reveal the seismic behavior of the embankment, but few of them have been done under a high confining stress.

A centrifugal model test is a test method which can simulate the same stress condition in a scaled model ground as in an actual ground. It has been applied to a dynamic problem using an earthquake simulator(Schofield 1981, Koga 1988).

This paper deals with the effects of the shape of the shaking acceleration on the excess pore pressure in the ground and on the settlement of the embankment. The applicability of a cumulative damage concept in equalizing the irregular shaking wave is discussed.

2 TEST PROCEDURE

Embankment models and horizontal layer models as shown in Fig.1 were made in a rigid soil container of 80cm in length, 30cm in height and 10cm in width.

A sand layer was prepared by pouring Toyoura sand through air. The surface of the layer was rounded in accordance with a rotational radius.

After setting the container in a vacuum box the sand layer was saturated with silicone oil which is 30 times as viscous as water. An embankment was made of a mixture of Toyoura sand and a clay-sand which has a ratio of 4:1 in weight and a water content of 15%.

A horizontal shaking was conducted with a centrifugal acceleration of 30g. Response accelerations, excess pore pressures and a settlement of the embankment were measured by transducers located as in Fig.1. Test condition is summarized in Table 1. In every model, the amplitude of 1st shaking acceleration was stepwise increased for respective cases to examine the seismic behavior of the model against different shaking levels. Sinusoidal waves of 60 Hz and 100Hz, and two kinds of irregular waves were used as the shaking acceleration. The shapes of these shaking waves are shown in Fig.2.

3 METHOD OF DATA ARRANGEMENT AND CALCULATION

The calculation procedure is as follows.

3.1 Equivalent Shaking Acceleration

An equivalent shaking acceleration for the cases using irregular waves was calculated based on a cumulative damage concept. The procedure of the calculation is shown in Fig.3.

1) Calculation of Dynamic Shear Stress Ratio

The effective overburden pressure σ_{vo}' and the dynamic shear stress ratio τ_d/σ_{vo}' were calculated one-dimensionally at a point where the pore pressure transducer was installed (P1 to P6).

Although the response acceleration was amplified or reduced due to liquefaction, it was assumed to be the same as the shaking acceleration for simplicity.

2) Assumption of Liquefaction Resistance Curve

The liquefaction resistance curve was assumed to be given by the equation in Fig.4, which was determined referring to the liquefaction resistance curve of Toyoura sand obtained from cyclic torsion shear tests.

Above equation can be rewritten as

$$N_C/N' = f\ (\tau_d/\sigma_{mo}') \quad (1)$$

in which f = equation to give the relation between cyclic stress ratio and normalized number of cycles.

3) Calculation of Damage Factor

When the irregular train of the dynamic stress ratio is divided into every half cycle, the damage factor D up to the i-th half cycle is defined in the cumulative damage concept as

$$D = \Sigma_i \frac{0.5}{(N_C)i} \quad (2)$$

in which $(N_C)i$ = number of cycles to cause liquefaction when the i-th half cycle stress ratio $(\tau_d/\sigma_{mo}')i$ is repeatedly applied.

The damage factor was calculated from the equation below, which was obtained by substituting Eq.(1) into Eq.(2).

$$D = \frac{1}{N'} \cdot \Sigma_i \frac{0.5}{f\{(\tau_d/\sigma_{mo}')_i\}} \quad (3)$$

4) Calculation of Equivalent Shaking Acceleration

If a uniform cyclic shear stress of 20 cycles is applied to give the same cumulative damage as the irregular wave, the amplitude of the equivalent shear stress ratio $(\tau_d/\sigma_{mo}')_{eq}$ can be calculated from the equation below.

$$D = \frac{1}{N'} \cdot \Sigma_i^{20} \frac{0.5}{f\{(\tau_d/\sigma_{mo}')_{eq}\}} = \frac{20}{N' \cdot f\{(\tau_d/\sigma_{mo}')_{eq}\}} \quad (4)$$

Combining Eqs.(3)&(4) the equivalent shear stress $(\tau_d/\sigma_{mo}')_{eq}$ can be obtained. After converting the effective mean stress σ_{mo}' into the effective overburden pressure σ_{vo}', the equivalent shaking acceleration A_{eq} was calculated from the following equation.

$$(\tau_d/\sigma_{vo}')_{eq} = \frac{1}{\sigma_{vo}'} \cdot A_{eq} \cdot \Sigma_i \frac{\gamma i \cdot h i}{g} \quad (5)$$

The coefficient of equalization C_{eq} was defined and calculated as

$$C_{eq} = \frac{A_{eq}}{A_{max}} \quad (6)$$

in which A_{max} is the maximum amplitude of the shaking acceleration before the equalization.

The relationship between the equivalent shaking acceleration A_{eq} and the settlement of the embankment for the cases using irregular waves was arranged to compare with the ones for the cases using the sinusoidal waves. The relationship between the equivalent shaking acceleration A_{eq} and the excess pore pressure in the ground was also compared in the same way.

3.2 Liquefaction Resistance Factor

1) Calculation of Liquefaction Resistance

The possible range of the parameter N' in Fig.4 which locates the liquefaction resistance curve was estimated so that the calculated damage factor D by Eq.(3) agrees with the experimental results whether the liquefaction occurred or not in the free ground.

2) Calculation of Liquefaction Resistance Factor

A liquefaction resistance factor F_L is defined as

$$F_L = \frac{R}{L} \quad (7)$$

in which R is the dynamic shear resistance ratio, L is the shear stress ratio during earthquakes.

An equivalent liquefaction resistance factor F_{Li} up to the i-th half cycles was defined as well by the following equation.

$$F_{Li} = \frac{R_{20}}{L_i} \quad (8)$$

in which R_{20} is the dynamic shear resistance ratio corresponding to a uniform wave of 20cycle, L_i is the equivalent shear stress ratio up to the i-th half cycles.

The shear resistance ratio R_{20} was computed by substituting the estimated value of N' and the number of cycles N_C = 20 into the equation in the Fig.4.

The equivalent shear stress ratio L_i was computed in the same way as was used to derive $(\tau_d/\sigma_{mo}')_{eq}$ in the preceding section using the estimated value of N'.

The relationship between the liquefaction resistance factor F_{Li} and the excess pore pressure ratio r_u was arranged for every pore pressure data to investigate the effect of the embankment on the relationship.

4 RESULTS AND DISCUSSIPONS

4.1 Equivalent Shaking Acceleration

Table 2 shows the equivalent shaking accelerations and the coefficient of equalization for the first shaking steps of embankment models using an irregular wave.

The coefficient of equalization below the embankment were mostly larger than in the free field.

The coefficients of equalization for the cases using an irregular wave of a high frequency were generally larger than those for the cases using an irregular wave of a low frequency, because the number of waves with a large amplitude was larger in the former than in the latter.

In the following the equivalent shaking acceleration at a middle point below the embankment (P5) is used as a representative value.

4.2 Settlement of Embankment

Fig.5 shows the relationship between the settlement of embankment and the shaking acceleration in the first shaking steps, where the shaking acceleration was defined to be a maximum amplitude in the irregular shakings and an average amplitude in the sinusoidal shakings. The settlement for the same shaking acceleration was larger for the cases using the sinusoidal wave than for the cases using the irregular wave.

On the contrary the relationship between the settlement and the equivalent shaking acceleration was almost similar irrespective of the shaking waves as is shown in Fig.6. This result indicates the effectiveness of the cumulative damage concept in equalizing the irregular shaking wave.

As for the effect of the frequency, the shaking using a sinusoidal wave of 60Hz caused a larger settlement than the shaking using that of 100Hz . It may be caused by a larger amplitude of a cyclic displacement and a longer duration for the sinusoidal shaking of a lower frequency. A series of shaking table tests conducted by one of the authors showed a similar result(Koga 1990). Such effect of the frequency cannot be considered in the process of the equalization based on the cumulative damage concept except the frequency-dependent characteristics of the response acceleration.

4.3 Excess Pore Pressure in Ground

Fig.7 shows the relationship between the maximum excess pore pressure ratio in the ground and the equivalent shaking acceleration in the first shaking steps of the embankment models. It was almost similar irrespective of the shaking waves both in the free ground and below the embankment. Only the results of P3 and P6 are shown. This result indicates the cumulative damage concept was effective in equalizing the irregular shaking wave for the excess pore pressure in the ground as well.

4.4 Liquefaction Resistance in Free Ground

The estimated N' to locate the liquefaction resistance curve was almost in the range from 1 to 3, and the dynamic shear resistance ratio R_{20} was almost in the range from 0.16 to 0.21. They were not much affected by the shaking wave. These results indicate the effectiveness of the cumulative damage concept in estimating the liquefaction resistance of the ground.

4.5 Relationship between Liquefaction Resistance Factor and Excess Pore Pressure Ratio

The relationship between the liquefaction resistance factor F_{L1} and the excess pore pressure ratio r_u of the horizontal layer models is shown in Fig.8, and that of the embankment models is shown in Fig.9. In the calculation the estimated N' was used for the horizontal layer models, and for the embankment models N' was assumed to be 2 which is a representative value of horizontal layer models. In the embankment models the point P4 just below the embankment was excluded from the data arrangement, because the excess pore pressure at the point was negative during the shaking. The results can be summarized as follows.

(1) In the horizontal layer the excess pore pressure ratio at shallow points P1 and P4 was similar to F_L^{-2}, and the one at the other deep points was similar to F_L^{-7}. The horizontal location of the points did not affect the relationships (Comparison between P1 to P3 and P4 to P6 in Fig.8).

(2) Below the embankment (P5 and P6 in Fig.9) the excess pore pressure ratio for the same value of F_L was smaller than in the free ground (P1 to P3 in Fig.9).

(3) The effect of the shaking history and that of the shape of the shaking wave on the results of (1) and (2) were small(Figs.8 and 9).

5 CONCLUSION

(1) The cumulative damage concept was effective in equalizing an irregular shaking wave to evaluate the excess pore pressure in the sand layer and the settlement of the embankment.

(2) The excess pore pressure ratio for the same liquefaction resistance factor was larger in the free field than below the embankment. It was the largest near the surface of the free field.

REFERENCES

Koga, Y., Taniguchi, E., Koseki, J. and Morishita, T. 1988 : Sand Liquefaction Tests Using a Geotechnical Dynamic Centrifuge, Proc. of the 20th Joint Meeting of U.S. -JAPAN Panel on Wind and Seismic Effects, U.S. -JAPAN Conference on Development and Utilization of Natural Resources.

Koga, Y. and Matsuo, O. 1990 : Shaking Table Tests of Embankments Resting on Liquefiable Sandy Ground, Soils and Foundations, Vol.30, No.4, pp.162-174.

Schofield, A.N. 1981 : Dynamic and Earthquake Geotechnical Centrifuge Modelling, Proc. Int. Conf. Recent Advances in Geotechnical Earthquake Engineering and Soil Dynamics.

Table 1 Test Cases and Conditions

Model	Case	Type of Model Ground	Shaking Wave 1st Shaking Acc.(g)*
A	A-1 ～A-6	Embankment	Sinusoidal,60Hz, 20cycle / 1.2～9.0
B	B-1 ～B-3	Horizontal Layer	Sinusoidal,60Hz, 50cycle / 2.3～4.5
C	C-1 ～C-3	Embankment	Sinusoidal,100Hz, 20cycle / 4.0～8.9
	C-4 ～C-6	Embankment	Irregular High Frequency / 4.3～8.3
	C-7 ～C-9	Embankment	Irregular Low Frequency / 5.4～8.7
D	D-1 ～D-2	Horizontal Layer	Sinusoidal,100Hz, 20cycle / 3.4,3.9
	D-3 ～D-4	Horizontal Layer	Irregular High Frequency / 4.9,8.1
	D-5 ～D-6	Horizontal Layer	Irregular Low Frequency / **,6.7

* An average amplitude is shown for sinusoidal shakings, and the maximum amplitude for irregular shakings.

** The shaking acceleration was not known due to mismeasurement.

***The relative density of the sand layer was about 57～68%.

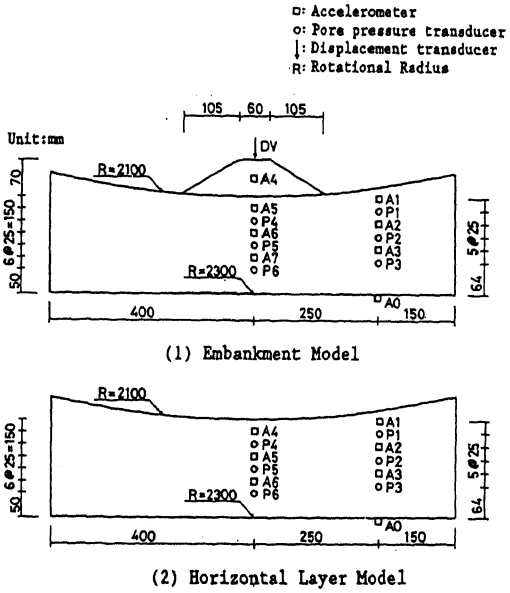

(1) Embankment Model

(2) Horizontal Layer Model

Fig.1 Test Models and Location of Transducers

Table 2 Equivalent Shaking Accelerations and Coefficients of Equalization

Cace	Shaking Wave	Equiv.Shaking Acc.Aeq (g) / Coef.of Equalization Ceq			
		Free Ground*	at P4	at P5	at P6
C-4	Irregular	3.0/0.50	3.8/0.64	3.6/0.61	3.5/0.59
C-5	High	6.8/0.82	4.7/0.57	5.6/0.68	6.2/0.75
C-6	Frequency	2.4/0.55	2.6/0.61	2.6/0.61	2.5/0.59
C-7	Irregular	2.5/0.47	3.2/0.59	3.0/0.56	3.0/0.55
C-8	Low	2.8/0.40	3.7/0.53	3.5/0.49	3.3/0.48
C-9	Frequency	3.7/0.42	4.1/0.48	3.9/0.44	3.7/0.42

* In the free ground Aeq and Ceq were the same irrespective of the depth,because the water level was equal to the surface of the sand layer.

(1) Sinusoidal Wave of 60Hz (20cycle)

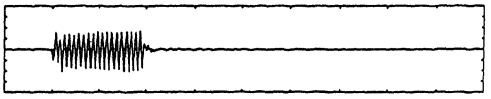

(2) Sinusoidal Wave of 100Hz (20cycle)

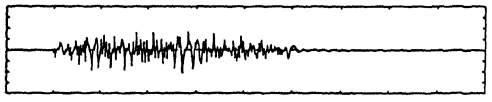

(3) Irregular wave of High Frequency

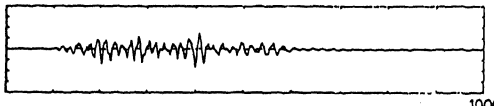

(4) Irregular wave of Low Frequency

1000 Time(msec)

Fig.2 Shape of Shaking Waves

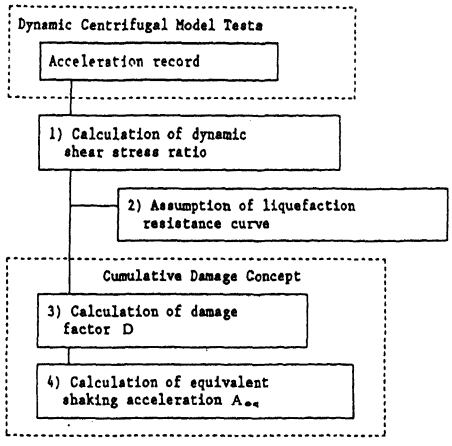

Fig.3 Procedure of Equalization

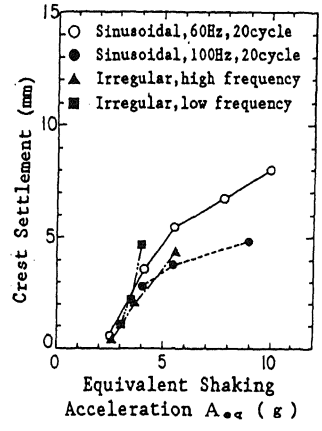

Fig.6 Equivalent Shaking Acc. vs. Crest Settlement

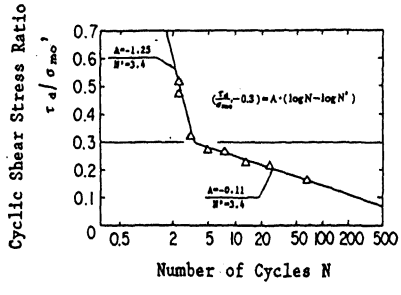

△ : Cyclic torsional shear test results
Toyoura sand, D_r= 55～60%
σ_{vo}'=1.0, σ_{ho}'=0.5(kgf/cm²)
Axial displacement confined
γ_{DA} = 15%
N'=parameter to locate liquefaction curve

Fig.4 Assumed Liquefaction Resistance Curve

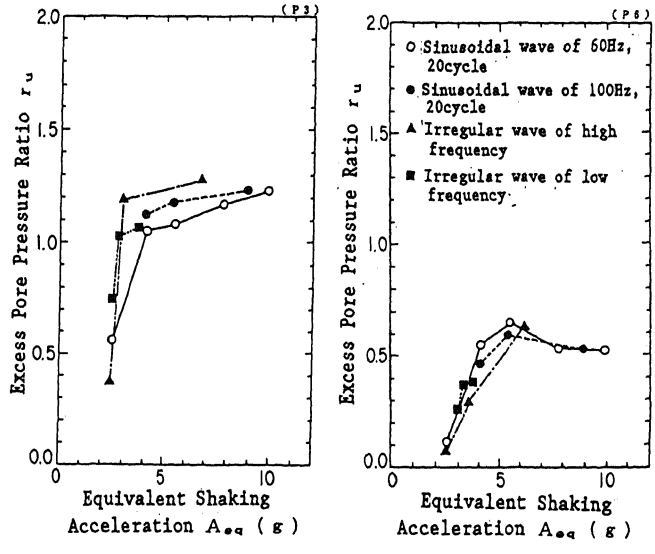

(1) at P3 (2) at P6

Fig.7 Equivalent Shaking Acc. vs. Excess Pore Press. Ratio (Embankment Models)

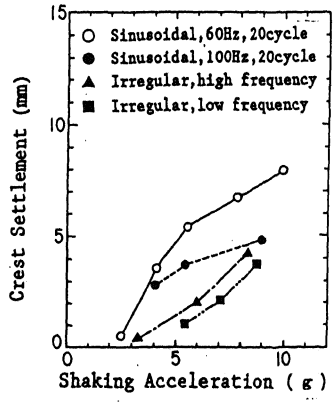

Fig.5 Shaking Acc. vs. Crest Settlement

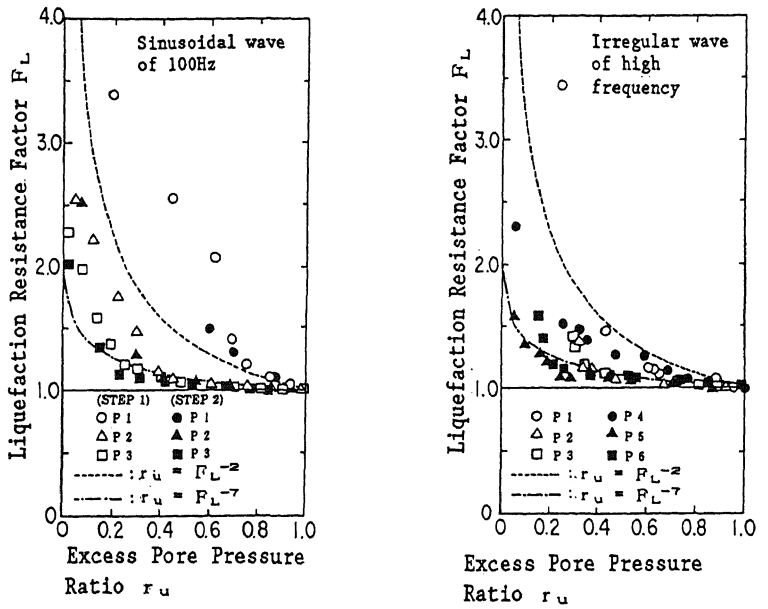

(1) Case D-2 , Step1 and Step2 (2) Case D-4 , Step1

Fig. 8 Liq. Resistance Factor vs. Excess Pore Press. Ratio (Horizontal Layer Models)

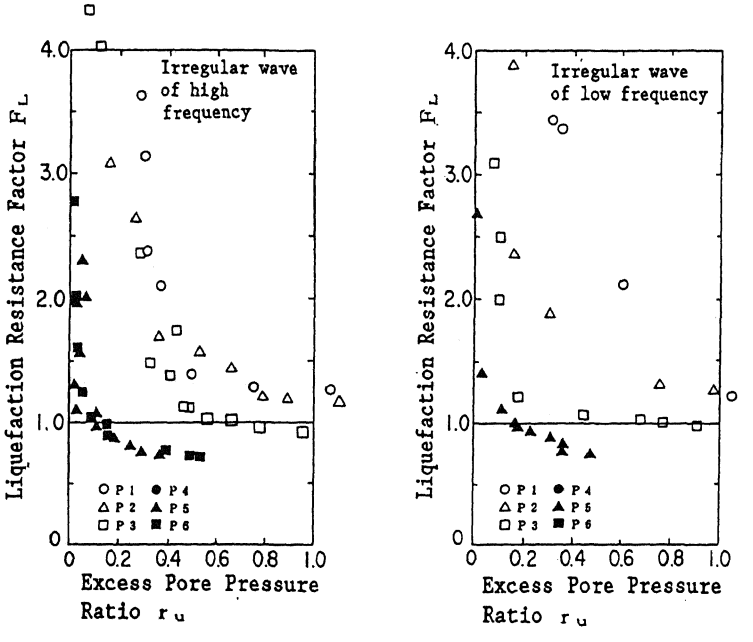

(1) Case C-4 , Step2 (2) Case C-9 , Step1

Fig. 9 Liq. Resistance Factor vs. Excess Pore Press. Ratio (Embankment Models)